GEOPHYSICS, VOL. 52, NO. 5 (MAY 1987); P. 644-654, 12 FIGS., 3 TABLES.

The dielectric constant of sandstones, 60 kHz to 4 MHz

Rosemary J. Knight* and Amos Nur*

ABSTRACT

Complex impedance data were collected for eight sandstones at various levels of water saturation (S_w) in the frequency range of 5 Hz to 4 MHz. The measurements were made using a two-electrode technique with platinum electrodes sputtered onto the flat faces of disk-shaped samples. Presentation of the data in the complex impedance plane shows clear separation of the response due to polarization at the sample-electrode interface from the bulk sample response. Electrode polarization effects were limited to frequencies of less than 60 kHz, allowing us to study the dielectric constant κ' of the sandstones in the frequency range of 60 kHz to 4 MHz.

κ' of all samples at all levels of saturation shows a clear power-law dependence upon frequency. Comparing the data from the eight sandstones at $S_w = 0.36$, the magnitude of the frequency dependence was found to be proportional to the surface area-to-volume ratio of the pore space of the sandstones. The surface area-to-volume ratio of the pore space of each sandstone was determined using a nitrogen gas adsorption technique and helium porosimetry.

κ' also exhibits a strong dependence on S_w. κ' increases rapidly with S_w at low saturations, up to some critical saturation above which κ' increases more gradually and linearly with S_w. Using the surface area-to-volume ratios of the sandstones, the critical saturation in the dielectric response was found to correspond to water coverage of approximately 2 nm on the surface of the pore space. Our interpretation of the observed dependence of κ' on both frequency and S_w is that it is the ratio of surface water to bulk water in the pore space of a sandstone that controls the dielectric response through a Maxwell-Wagner type of mechanism.

INTRODUCTION

The dielectric constant, or relative permittivity, of a material is the permittivity of the material normalized with respect to the permittivity of a vacuum. The complex dielectric constant κ^* can be written as $\kappa^* = \kappa' - i\kappa''$, where κ' is the real part and κ'' is the imaginary part of the complex dielectric constant. While the measured values of both κ' and κ'' are related to material properties, the use of κ' as a diagnostic parameter in well logging has become a subject of great interest over the past ten years. We present the results of a laboratory study of κ' of eight sandstones in the frequency range of 60 kHz to 4 MHz whose principal aim was the dependence of κ' on frequency and the level of water saturation in the pore space.

The quantity κ' is a measure of the amount of polarization in a material. There can be a number of different polarizing species or mechanisms present, each having a characteristic relaxation frequency and an associated dielectric dispersion centered around this relaxation frequency. Figure 1 (modified after Poley et al., 1978) illustrates the dispersions of κ' that theoretically are found in a material in the frequency range of 10^3 to 10^{15} Hz. At the highest frequencies, the polarizing species in a material are the electrons. At frequencies below about 10^{13} Hz, there is also a contribution from atomic polarization. Dipolar polarization, the orientation of polar molecules, occurs at frequencies below about 10^{10} Hz. At frequencies below about 10^5 Hz, various types of charge polarizations occur, all of which are collectively referred to in this study as Maxwell-Wagner mechanisms (Maxwell, 1891; Wagner, 1914).

The values of the dipolar dielectric constant initially sparked interest in using the dielectric constant as a well-logging tool for formation evaluation. Table 1 illustrates the potential usefulness of the dipolar dielectric constant as a means of measuring the level of water saturation (Poley et al., 1978). The dipolar dielectric constant of water is 80, significantly different from that of the rock matrix (approximately 6) or that of oil (2.2) or gas (1). It was hoped that by using a simple mixing law, the level of water saturation could be determined from the measurement of κ'.

Manuscript received by the Editor September 26, 1985; revised manuscript received September 4, 1986.
*Department of Geophysics, Stanford University, Stanford, CA 94305.

In the study reported here we have determined κ' for eight sandstones at various levels of water saturation in the frequency range of 60 kHz to 4 MHz. We found κ' of saturated sandstones to be strongly dependent upon frequency, a result previously reported by others, such as Keller and Licastro (1959), Scott et al. (1967), Poley et al. (1978), and Lockner and Byerlee (1985). In addition to this frequency dependence, we found two distinct regions in the dependence of κ' on saturation. We consider both the frequency dependence and the saturation dependence in terms of the microgeometry of the pore space and its effect on the contained water.

SAMPLE DESCRIPTION

The eight sandstones used in this study are described in Table 2. The porosities, permeabilities, and petrographic descriptions are taken from the Stanford Rock Physics Rock Catalogue. Porosities were determined using a helium porosimeter; the permeability values were determined using steady-state brine flow tests; the petrographic description of each sandstone is based on a 400 point count analysis of the thin section. The samples range in porosity from 0.065 to 0.275, with permeability ranging from 2 μD to 950 mD, and volume fraction of clay ranging from 0.00 to 0.18. The three samples of Berea sandstone all have porosities of approximately 0.2 and differ mainly in permeability and clay content. Samples CH58-79, CH61-79, and CH66-79 are tight gas sandstones from the Spirit River formation in the Alberta basin. These samples have very low porosity and permeability with a considerable amount of carbonate cement and a high clay content, in the form of argillaceous lithics and as a clay cement. St. Peter's sandstone is an orthoquartzite, with essentially no clay and a porosity of 0.173. Indiana Dark is a high-porosity sandstone with a cement dominated by iron oxides.

As a means of characterizing the microgeometry of the pore space of the sandstones in this study, we determined surface area-to-volume ratios of the internal pore space of the samples. The surface areas were obtained from nitrogen adsorption isotherms by using the Brunauer-Emmett-Teller (BET) equation (Brunauer et al., 1938). Although it was necessary to break the samples into pieces that could fit through a funnel 4 mm in diameter, care was taken to avoid totally crushing the sample, so that the geometry of the pore space could be preserved.

The total adsorption isotherm of one of the samples (CH66-79) is shown in Figure 2. This isotherm is an example of a Type II adsorption isotherm which is characteristic of adsorption in microporous solids (Brunauer et al., 1940). The surface area was calculated from data in the linear portion of the plot, $0.05 < P_e/P_s < 0.3$, where P_e is the equilibration pressure and P_s is the saturation vapor pressure of nitrogen.

The surface area of a sandstone is a measure of the total area of the interface between the minerals and the pore space. In a sandstone composed entirely of quartz grains, the surface area depends upon the shape of the individual pores. A simple calculation will show, however, that a small amount of material with a large surface area added to such a sandstone will significantly increase the surface area; so while pore geometry is a contributing factor to surface area, the most important factor in sandstones is the percentage of material with high surface area. The following are examples of such materials commonly found in sandstones and their surface areas. Kaolinite has a measured surface area of 10.6 to 70 m^2/g (Ormsby and Shartsis, 1960); illite has a measured surface area of 52 to 82 m^2/g (Johansen and Dunning, 1959); montmorillonite has a measured surface area of 282 to 491 m^2/g (Orchisrtron, 1955); geothite has a surface area of 32 m^2/g (Gast et al., 1974); and amorphous iron oxide has a surface area of 320 m^2/g (Gast et al., 1974).

The values for surface area determined for the sandstone samples are given in Table 3. Values range from 0.124 m^2/g for St. Peter's (a clean orthoquartzite) to 5.00 m^2/g for Indiana Dark (which has 22 percent iron oxides and hydroxides). The value of 1.23 m^2/g determined for Berea 100 is in excellent agreement with the value of 1.25 m^2/g determined by Hawkes and Mellor (1970) from nitrogen adsorption.

Surface area per unit volume of pore space was calculated

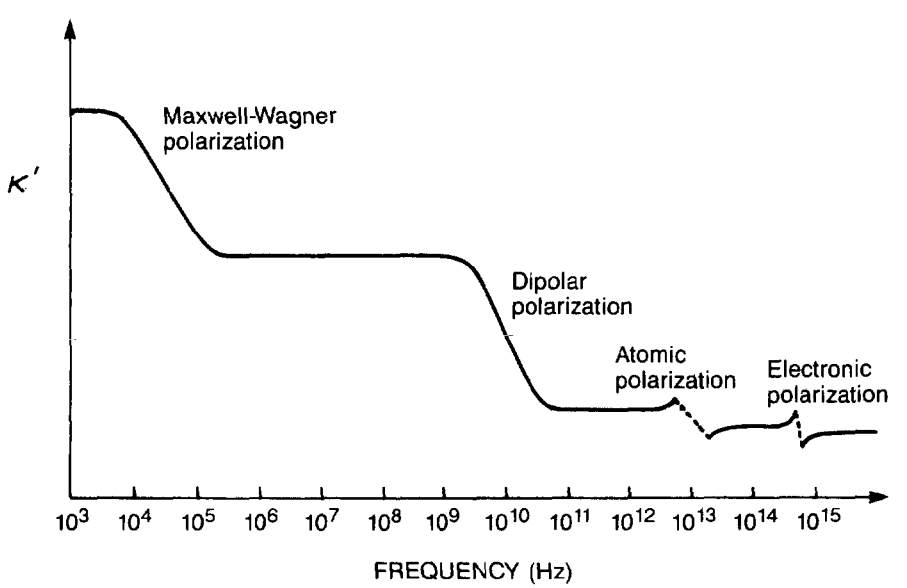

FIG. 1. Dielectric dispersion of various types of polarization (modified after Poley et al., 1978).

as

$$\frac{\text{surface area}}{\text{volume}}\,(\text{cm}^{-1}) = \frac{\text{surface area}}{\text{mass}}\left(\frac{\text{m}^2}{\text{g}}\right) \times 2.64\left(\frac{\text{g}}{\text{cm}^3}\right) \times \left(\frac{1-\phi}{\phi}\right) \times 10^4\left(\frac{\text{cm}^2}{\text{m}^2}\right),$$

where ϕ is porosity and the density of the solid component of the sandstone is assumed to be 2.64. These surface area-to-volume ratios are also listed in Table 3. Samples CH58-79, CH61-79, and CH66-79 are tight gas sandstones; their relatively high surface areas and low porosities result in their having the highest ratios of surface area to volume of the sandstones in this study.

EXPERIMENTAL PROCEDURE

Measurement of the electrical properties of a material can be made in either the series or parallel mode. In the series mode, the complex impedance Z^* is measured,

$$Z^* = R_s - iX_s,$$

where R_s is the series resistance and X_s is the reactance. The complex resistivity ρ^* can be calculated from Z^*,

$$\rho^* = Z^* \frac{A}{t},$$

where A is the cross-sectional area of the sample and t is its thickness.

In the parallel mode, the complex admittance Y^* is measured,

$$Y^* = (Z^*)^{-1}$$

and

$$Y^* = G_p + iB_p,$$

where G_p is the conductance and B_p is the susceptance. The complex conductivity σ^* and the complex dielectric constant κ^* can be calculated from Y^*,

$$\sigma^* = Y^* \frac{t}{A}$$

and

$$\kappa^* = \frac{Y^*}{i\omega\varepsilon_0}\frac{t}{A},$$

where ω is angular frequency and ε_0 is the permittivity of a vacuum, $\varepsilon_0 = 8.85 \times 10^{-12}$ F/m.

Complex impedance data were collected with an HP4192A impedance analyzer over the frequency range of 5 Hz to 4 MHz. Disk-shaped samples were used with a diameter of 5.1 cm and a diameter-to-thickness ratio of greater than 10:1; this geometry ensures that errors due to stray capacitance are negligible (Scott and Curtis, 1939). Electrodes were applied by sputtering 100 nm of platinum onto the opposite flat faces of the disk-shaped samples (sputtering is an excellent way of ensuring good contact with a sample regardless of the degree of

Table 1. κ' of materials commonly encountered in formation evaluation.

Substance	κ'
Quartz	4.5–4.7
Calcite	7–8
Shale	13–15
Gas	1
Oil	2.2
Water	80

Table 3. Surface area, surface area-to-volume ratio, and the power-law exponent α for the eight sandstones in this study.

Sample	Surface area (m^2/g)	S/V (cm^{-1})	α
St. Peter's	0.124	1.57×10^4	0.080
Berea 200	0.840	8.40×10^4	0.140
Berea 400	0.968	8.90×10^4	0.172
Berea 100	1.234	1.33×10^5	0.158
Indiana Dark	5.00	3.48×10^5	0.150
CH58-79	2.07	7.38×10^5	0.245
CH66-79	2.65	1.01×10^6	0.266
CH61-79	2.97	1.04×10^6	0.251

Table 2. Sample description.

			Petrographic description (as % total)							
			Framework grains				Cements			
Sample	ϕ	k	quartz	chert	feld-spar	lithics	quartz	clay	iron oxide	carbon-ates
Berea 100	.197	84 mD	53	2	3	8	11	7(c)	—	7
Berea 200	.209	372 mD	58	1	7	8	10	3	—	1
Berea 400	.219	397 mD	61	2	6	2	8	1(c)	—	1
CH58-79	.069	10.30 μD(a)	30	12	—	6	—	18	—	18
CH61-79	.070	7.18 μD(a)	38	16	1	4(b)	16	3	—	15
CH66-79	.065	2.38 μD(a)	30	12	—	6(b)	8	18	—	24
St. Peter's	.173	944 mD	77	—	—	—	8	—	—	—
Indiana Dark	.275	30.2 mD	57	—	7	—	—	5	22	—

ϕ = porosity; k = permeability. (a) in-situ conditions, (b) argillaceous, (c) clay percentage includes minor chlorite and/or sericite.

water saturation of the sample). The sample holder was constructed of Plexiglas and was connected to the impedance analyzer through an HP 16047A test fixture. The HP 4192A has a zero-offset option which can be used to correct for impedance contributions from the sample holder, test fixture, and measurement circuit. This correction was made by first measuring the impedance of the measurement system short circuited across the sample and then measuring the impedance with the circuit open. As a test of the accuracy of the experimental setup, we prepared a sample from a material of known dielectric constant. The material is STYCAST HiK, manufactured by Emerson and Cuming (technical bulletin 5-2-2) which has a dielectric constant of 15 across the frequency range used here. The dielectric constant of this control sample was measured prior to any series of measurements. From this procedure the accuracy of the measurement was determined to be within 2 percent.

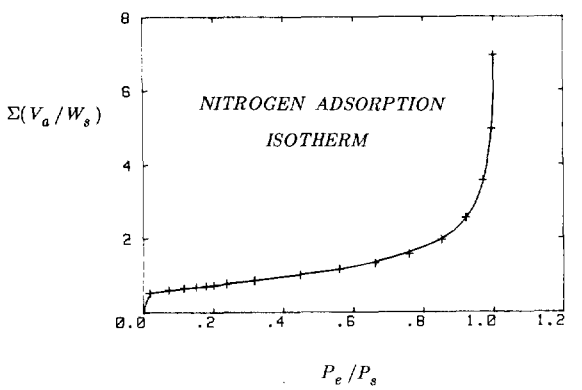

FIG. 2. Nitrogen adsorption isotherm for sample CH66-79. V_a is the volume of adsorbed gas, W_s is the sample weight, P_e is the equilibration pressure, P_s is the saturation vapor pressure of nitrogen.

The use of a two-electrode technique with blocking metallic electrodes resulted in polarization at the sample-electrode interface at low frequencies. A complex impedance plot clearly shows, however, the various components in the frequency response and allows separation of polarization at the sample-electrode interface from the bulk sample response (Knight, 1983). Figure 3 shows the Z^* plot of data from a partially saturated sample of Berea 100 sandstone where the negative reactance ($-X_s$) is plotted against the series resistance (R_s). As shown, frequency increases down the line and counterclockwise across the semicircle; we define the frequency separating the low-frequency linear response from the high-frequency semicircular response as f_0. This form of Z^* plot, composed of a depressed semicircular arc and an inclined straight line, is typical of the Z^* plots we obtained for all fully saturated and partially saturated samples and has been found in many studies of ionic conductors with blocking electrodes (Armstrong et al., 1972; Raistrick et al., 1976; Raistrick et al., 1977; De Bruin and Badwal, 1978). The low-frequency linear portion has been identified as the response of the sample-electrode interface, the high-frequency portion has been identified as the bulk sample response, and the value of R_s at f_0 has been identified as the bulk sample resistance (Raistrick et al., 1976; Raistrick et al., 1977). We have applied this interpretation to the complex impedance data of sandstones using only those data above f_0 as a measure of the bulk sample properties. We have found f_0 to be inversely proportional to the resistivity of the sample; because of this dependence of f_0 on resistivity, the low-frequency portion of the complex impedance plot which corresponds to polarization at the sample-electrode interface is not seen for dry samples. f_0 for saturated sandstones usually lies between 1 and 50 kHz.

The effect of water saturation on κ' was a major part of this study. A sample was fully saturated by initially evacuating it in a pressure vessel, then allowing degassed, deionized water

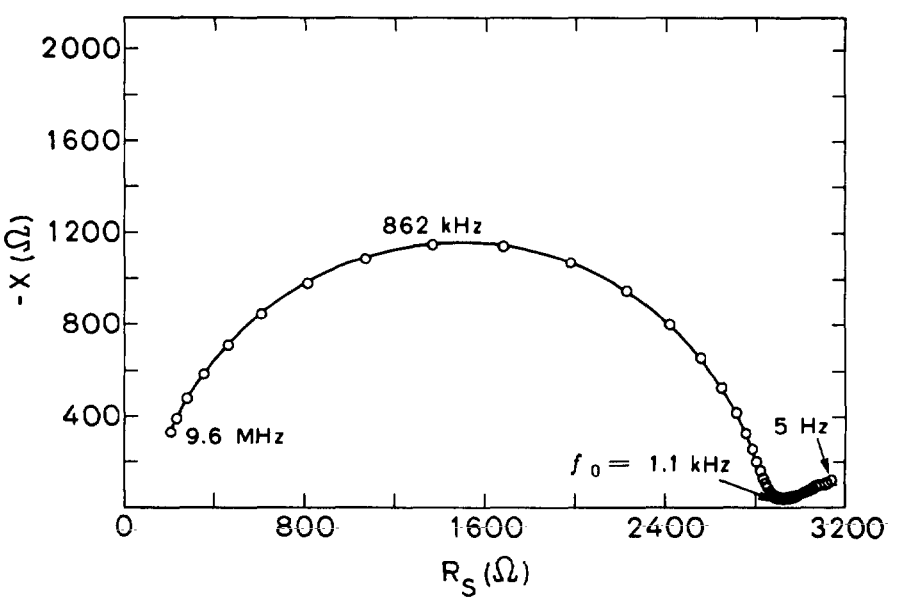

FIG. 3. Complex impedance plot of data from a partially saturated sample of Berea 100.

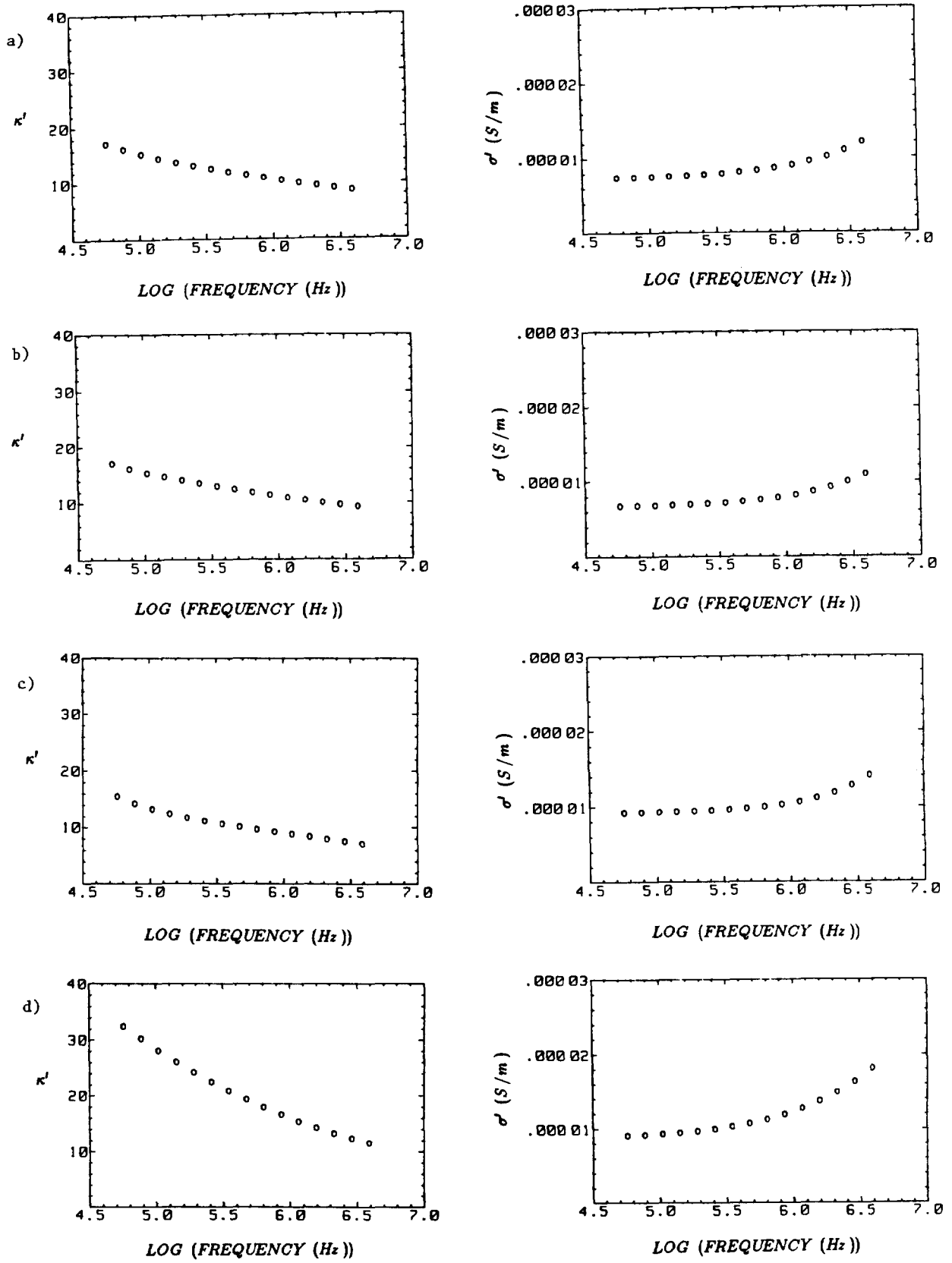

FIG. 4. κ' versus log frequency and σ' versus log frequency for the eight sandstones; $S_w = 0.36$ with deionized water. (a) Berea 100, (b) Berea 200, (c) Berea 400, (d) CH58-79.

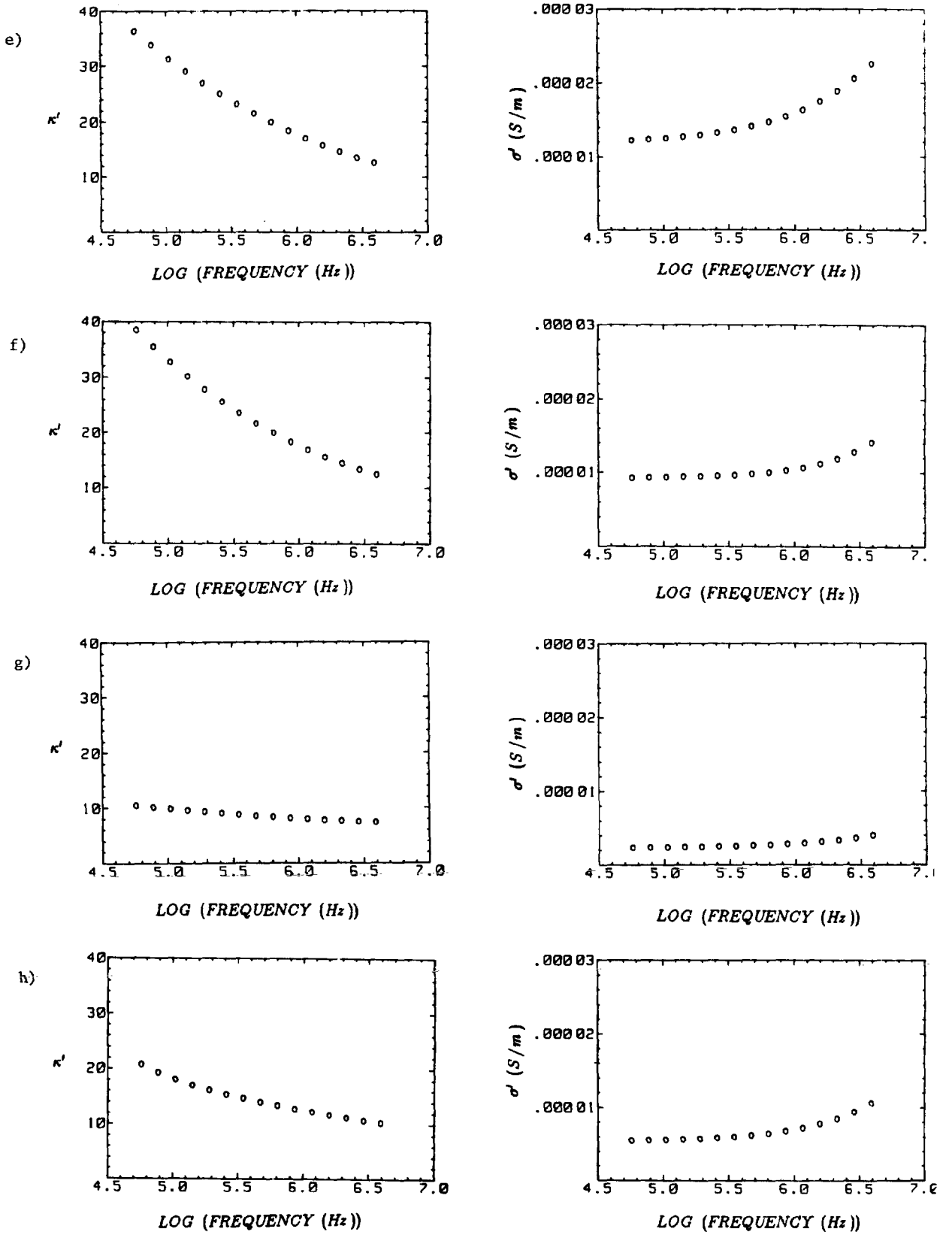

FIGS. 4e-4h. (e) CH61-79, (f) CH66-79, (g) St. Peter's, (h) Indiana Dark.

to flow into the vessel, thus saturating the sample under a confining pressure of 1 600 psi for at least 12 hours. Measurements on the fully saturated sample were made immediately after it was removed from the pressure vessel. Subsequent measurements were made as the sample dried, and its weight was being monitored to determine the level of water saturation. To obtain a partially saturated sample, the sample was soaked in a beaker containing water until the desired level of water saturation was reached.

Because the samples had been saturated previously in their natural environment with a pore fluid of some salinity, there could have been residual salts in the pores of the rock. These salts were removed by soaking the sample in deionized water, usually several weeks, until the sample was "salt-free." Because both σ' and κ' are sensitive to the salinity of the pore fluid, the samples were repeatedly dried, partially saturated with deionized water, and σ' and κ' were measured until the measured values of σ' and κ' at a set frequency were constant. At this point the sample was classified as salt-free; it was assumed that all residual salts had been removed so that deionized water could be put into the rock with confidence.

FREQUENCY DEPENDENCE

The Debye response (Debye, 1929) has frequently been used to describe dielectric dispersion in a system with a single relaxation time. However, many materials, including rocks, deviate from Debye behavior, suggesting the presence of a distribution of relaxation times. Examples of studies showing the non-Debye behavior of rocks are Saint-Amant and Strangway (1970), Alvarez (1973), Olhoeft (1974), Pelton (1978), Knight (1983), and Lockner and Byerlee (1985). The observed deviation from Debye behavior has led to modifications of the Debye equation, including the Cole-Cole expression and the corresponding Cole-Cole equivalent circuit (Cole and Cole, 1941). The significant feature of the Cole-Cole circuit is the inclusion of a constant-phase circuit element to model a distribution of relaxation times. The Cole-Cole expression has been found useful in fitting data from vacuum-dry lunar soil samples (Olhoeft, 1974), and an expression for Z^*, containing a term analogous to the constant-phase element in Cole and Cole (1941), has been used in modeling the impedance of mineralized rocks (Madden and Cantwell, 1967; Pelton, 1978).

In addition to the Cole-Cole expression, there are three other empirical expressions commonly used to describe a non-Debye response: the Cole-Davidson expression (Davidson and Cole, 1951), the combined Cole-Cole and Cole-Davidson expression (Davidson and Cole, 1951), and the Williams-Watkins expression (Williams and Watts, 1970). An interesting feature of all four empirical relations is that, at frequencies away from the relaxation frequency, they reduce to expressions showing a power-law dependence upon frequency of both κ' and κ'', which led Jonscher (1975) to define this power-law dependence of κ' and κ'' as the "universal dielectric response." Since κ' is the parameter of interest in this study, we now discuss the power-law dependence of κ' upon frequency.

Figure 4 shows κ' and corresponding σ' for the eight sandstones in this study, 36 percent saturated with deionized water. The frequency range in each case extends from 60 kHz to 4 MHz, 60 kHz being greater than the determined value of f_0 for all the samples. In this frequency range, κ' exhibits, in all the sandstones and at all levels of saturation, a power-law dependence upon frequency

$$\kappa' = A\omega^{-\alpha},$$

where A and α are constants that depend upon the sample and the level of saturation. The question is how the frequency dependence is related to rock properties. We are particularly interested in the relationship between α and the sample properties.

Figure 5 shows κ' as a function of frequency for five of the sandstones, all of which are 36 percent saturated with deionized water. The power-law dependence can be seen in this plot, with a different value of α for each sample. A power-law dependence in capacitance (from which κ' is calculated) has been observed in studies of a wide range of materials (Grahame, 1952; Scheider, 1975), and the microgeometry of the material was proposed in a number of cases to be the source of the frequency dependence (Grahame, 1952; Sarmousakis and Prager, 1957; de Levie, 1965; Scheider, 1975). We have found a relationship between the power-law exponent α (values listed in Table 3) and the microgeometry of a sandstone as characterized by the surface area-to-volume ratio of the pore space. Figure 6 gives a plot of the power-law exponent α for all the sandstones saturated to $S_w = 0.36$ with deionized water versus the surface area-to-volume ratio of the sample. These results suggest that in a partially saturated sandstone, the higher the surface area-to-volume ratio of the pore space, the greater the frequency dependence of κ'. Indiana Dark is one sandstone that deviates from this trend, possibly due to the high percentage of iron oxides and hydroxides in the sample and the effect of the magnetic susceptibility of these minerals on the dielectric response. In a review of dielectric data from a wide variety of materials, Jonscher (1979) defines limits for the power-law exponent in the frequency region of this study such that $0.4 < \alpha < 0$. It can be seen in Figure 6 that α falls within this range, asymptotically approaching 0.3 at high values of surface area-to-volume ratio.

Given that κ' is strongly dependent upon frequency in the range studied here and given the observed relationship between frequency dependence and surface area-to-volume ratio, we would expect κ' measured at any frequency between 60 kHz and 4 MHz to be proportional to the surface area-to-volume ratio. This is shown in Figure 7 where κ' of the eight sandstones, $S_w = 0.36$, measured at 140 kHz, is plotted as a function of the surface area-to-volume ratio. κ' increases as the surface area-to-volume ratio increases.

EFFECT OF THE LEVEL OF WATER SATURATION

We have shown that for a number of sandstones at the same level of water saturation, α is proportional to the surface area-to-volume ratio of the sample. When the level of water saturation in any one sample is varied, we find that α is also dependent upon S_w. Figure 8 shows the change in α with change in S_w for the tight gas sandstone sample, CH61-79. As the level of saturation in a sample decreases from fully saturated, α increases until some critical saturation point at low saturations below which α drops rapidly to near 0.

The presence of a critical saturation at low saturation in the

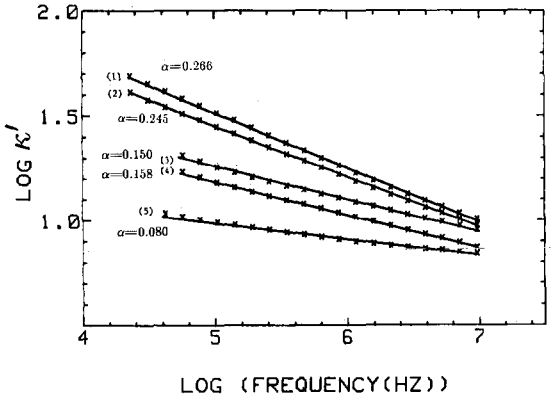

FIG. 5. Log κ' versus log frequency for five sandstones; S_w = 0.36 with deionized water. (1) CH66-79, (2) CH58-79, (3) Indiana Dark, (4) Berea 100, and (5) St. Peter's. The power-law exponent α for each sandstone is given on the plot.

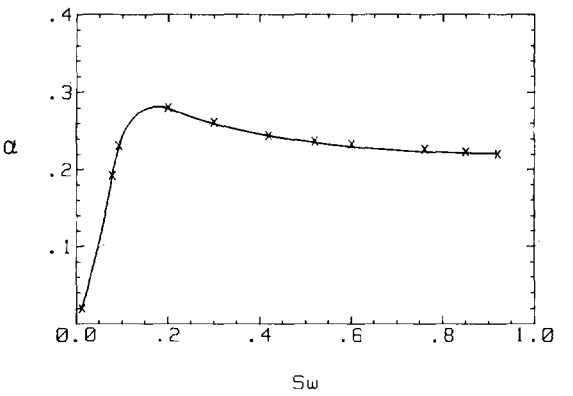

FIG. 8. The power-law exponent α versus S_w for sample CH61-79.

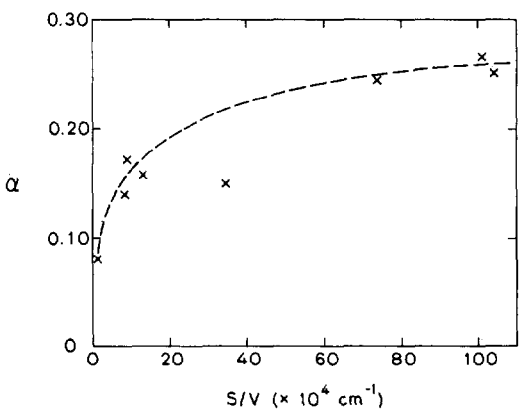

FIG. 6. α versus surface area-to-volume ratio for the eight sandstones; S_w = 0.36. Values of α with corresponding sample names are given in Table 3.

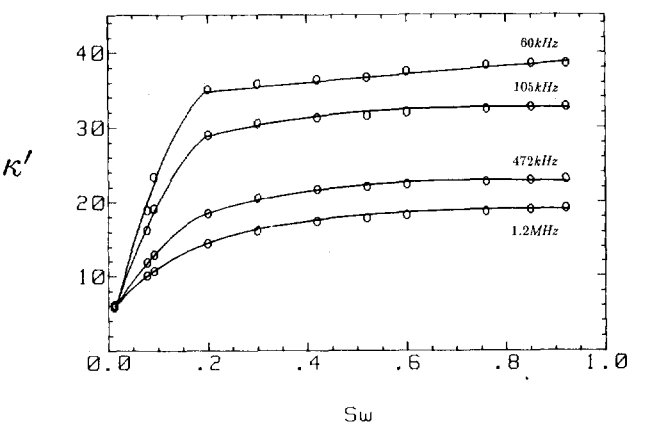

FIG. 9. κ' versus S_w for sample CH61-79 at four frequencies: 60 kHz, 105 kHz, 472 kHz, and 1.2 MHz.

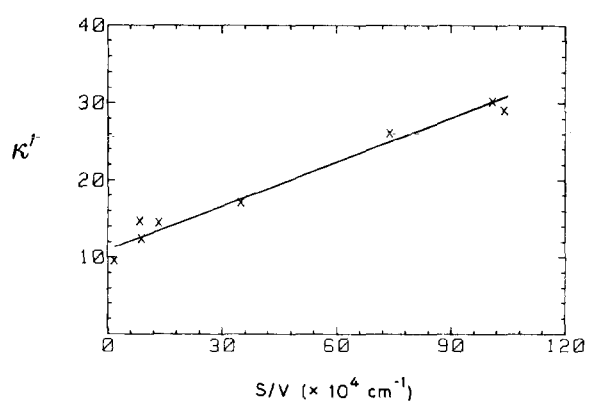

FIG. 7. κ' versus surface area-to-volume ratio for the eight sandstones; S_w = 0.36.

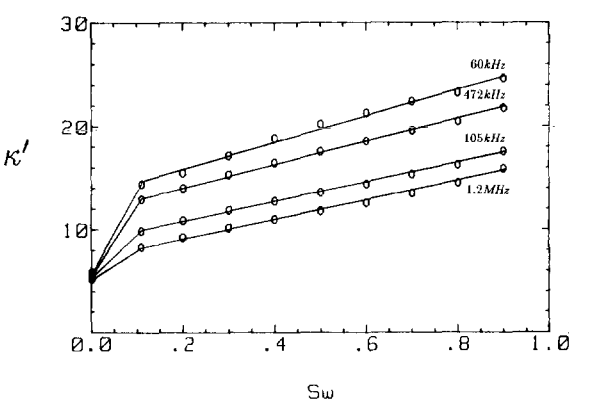

FIG. 10. κ' versus S_w for sample Berea 100 at four frequencies: 60 kHz, 105 kHz, 472 kHz, and 1.2 MHz.

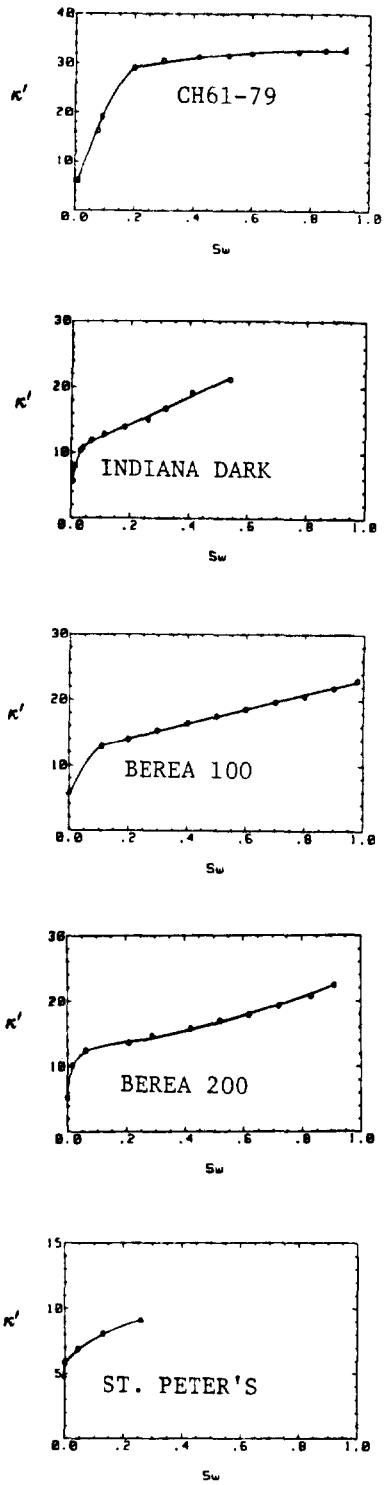

FIG. 11. κ' versus S_w at a frequency of 105 kHz for five sandstones: CH61-79, Indiana Dark, Berea 100, Berea 200, and St. Peter's.

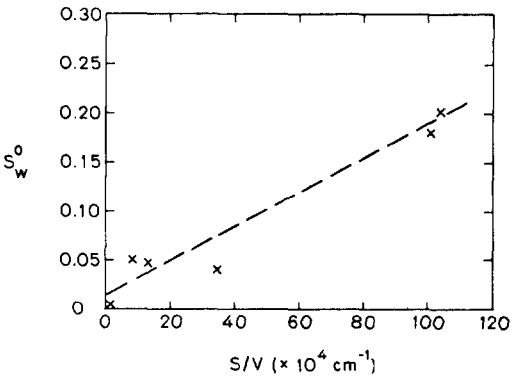

FIG. 12. S_w^0 calculated from the surface area-to-volume ratio of a sample, versus S_w^0 as seen in the dependence of κ' on S_w.

dielectric response of sandstones is obvious when we consider a plot of κ' as a function of S_w. Figure 9 shows κ' for CH61-79 versus S_w at various frequencies from 60 kHz to 4 MHz, and Figure 10 shows κ' for Berea 100 versus S_w. The observed dependence of κ' on S_w at these frequencies is linked to the strong frequency dependence. κ' increases rapidly up to some critical saturation S_w^0, then increases more gradually and linearly with increasing saturation.

Figure 11 shows κ' versus S_w at 105 kHz for five sandstones. There is a critical saturation point in the data for all the sandstones with a different value of S_w^0 for each sample. Consider the water in the pores of a rock as consisting of two phases, bulk pore water and a layer of water adjacent to the surface, several monolayers in thickness, that we will refer to as "surface water." We propose that the saturation level S_w^0 at which the dielectric constant becomes less sensitive to saturation is indicative of the amount of surface water in the rock. We interpret the variation of S_w^0 between samples as being due to differing amounts of surface water in different rocks. In other words, we anticipate that the internal surface area-to-volume ratio of the pore space, which determines the percent of surface water in a rock, should control the position of the break in κ' versus S_w.

Because of the low density of data, it is impossible to determine S_w^0 accurately. However, referring to Figure 11, some observations can be made. The tight gas sandstone, with relatively high surface area and low porosity, has a surface area-to-volume ratio of 9.45×10^5 per cm. S_w^0 for CH61-79 appears to be around 0.15. St. Peter's sandstone, by comparison, with very low surface area and high porosity, has a surface area-to-volume ratio of 1.57×10^{-4} per cm, and accordingly S_w^0 falls between 0.005 and 0.04. The data for the two Berea samples with surface area-to-volume ratios of 8.40×10^4 and 1.33×10^5 per cm suggest S_w^0's between 0.01 and 0.04. Indiana Dark, while being the sample with the highest surface area, also has the highest porosity, resulting in a surface area-to-volume ratio less than that of the tight gas sandstone, 3.48×10^5 per cm. S_w^0 for Indiana Dark falls in the range of 0.05 to 0.1. While more data in the region of S_w^0 are needed, the available data do suggest that the samples with high surface area-to-volume ratios contain a larger percentage of surface water in the pores and that this is reflected in the position of S_w^0.

We have calculated the amount of surface water expected in

these samples from the measured surface area-to-volume ratio using a thickness of 2 nm for the surface layer. The results shown in Figure 12 show fairly good correlation between S_w^0 predicted from this calculation and S_w^0 taken as the critical saturation point in the dependence of κ' on S_w.

DISCUSSION

We have found a power-law dependence of κ' upon frequency, with the power-law exponent proportional to the surface area-to-volume ratio of the pore space of a sandstone and the level of water saturation. The correlation we observed between α and the surface area-to-volume ratio of a sample can be extended to the observed changes with S_w if, instead of considering the surface area-to-volume ratio of the total pore space, we consider the ratio between the amount of surface water and the amount of bulk water in the volume of the pore space. In comparing different sandstones, the sample with the larger surface area-to-volume ratio of the pore space will have the larger amount of surface water relative to bulk water in the pore space, assuming that the thicknesses of the surface layers are the same in the different sandstones. α for the sandstones can thus be considered proportional to the ratio between the amounts of surface water and bulk water in the pore spaces of the different sandstones; those sandstones with a proportionately greater amount of surface water show a greater frequency dependence. In studying one sandstone at various levels of water saturation and considering the dependence of α on S_w, we suggest that the critical parameter is still the ratio between the amounts of surface and bulk water. As a rock dries, it is reasonable to assume that the surface water, being physically adsorbed to the pore surface, will remain, while the water in the central volume of the pore space is removed. This results in an increase in the ratio of the amount of surface water to the volume of bulk water in the pore space as the rock dries. We suggest that the maximum α occurs at a critical saturation where there is a maximum in the ratio of surface to bulk water; the drop in α below this saturation is due to removal of the surface water from the pore space. We conclude that there is a dielectric dispersion associated with the 2 nm of water adjacent to the surface of the pore space.

A number of examples in the literature focus on the role of surface water in the dielectric behavior of solid materials containing relatively small amounts of water (McIntosh et al., 1951; Kamiyoshi and Odake, 1953; Kurosaki, 1954; Thorp, 1959; Nair and Thorp, 1965a, 1965b; McCafferty and Zettlemoyer, 1971). The dielectric mechanism in each of these studies is interpreted either in terms of the rotational molecular mobility of individual water molecules or in terms of the larger scale conductivity heterogeneities in the water-solid system.

Water adjacent to a solid surface has a dielectric response significantly different from that of bulk water, most likely due to the reduction of molecular mobility of the water molecules through physical bonding to the surface (Kurosaki, 1954; Bockris et al., 1966; McCafferty and Zettlemoyer, 1971). Much evidence suggests that the restricted mobility reduces the static dielectric constant of water adsorbed to a surface from 80 for bulk water to close to 6 (Bockris et al., 1966). In addition to a reduced κ', data reviewed by Hasted (1961) indicate that surface bound water exhibits a relaxation in the region of 10 kHz, seven orders of magnitude lower that the relaxation frequency of bulk water. This has led to the suggestion that dielectric dispersion, at frequencies around 10 kHz in systems composed of a solid and adsorbed water, is due to the relaxation of the adsorbed water (McCafferty and Zettlemoyer, 1971).

An alternate form of interpretation is in terms of a Maxwell-Wagner type of mechanism (Maxwell, 1891; Wagner, 1914), in which the conductivity heterogeneities in a system are responsible for dielectric dispersion. With such a mechanism, it is not the rotational mobility of the water molecules in the surface water that is important, but the translational mobility, or the conductivity of the surface layer. A conductive mechanism has been proposed by Kamiyoshi and Odake (1953) and Nair and Thorp (1965a, 1965b), for dielectric dispersion in systems in which water coated the surfaces of a solid. Sen (1980) and Kenyon (1984) use a Maxwell-Wagner effect, modified by the shape of the grains, to explain the dielectric response of water-saturated sedimentary rocks.

In considering our data from sandstones at various levels of water saturation, we favor the interpretation that a conductive type of mechanism is responsible for the observed dielectric response. While both adsorbed water relaxation and a Maxwell-Wagner type of mechanism can explain the frequency dependence, the change in κ' with S_w suggests that a polarization other than the rotational molecular polarization of the water molecules is contributing to κ'. The dielectric constant of a dry sandstone is approximately 6; if the 2 nm of surface water is to be treated as bound water with a restricted molecular mobility and a dielectric constant of 6, then the addition of the surface water to the dry sandstone should have little effect on κ'. We observe, however, a rapid increase in κ' with the presence of the 2 nm of surface water. We attribute this apparently enhanced dielectric constant of the surface water to the role of the conductivity of the surface water in the dielectric response.

As a very simple physical model, we can think of the conductive coating of water on the surface of the grains in a sandstone as producing numerous water-grain capacitors, causing the sample to act effectively as a network of grain-size capacitors which contribute to the total measured κ'. A rapid increase in κ' with increasing S_w is observed as the conducting liquid film coats the pore space and the number of water-grain capacitors increases. At S_w^0, the pore surface is completely coated with a conducting film, and the maximum value in κ' due to the contribution from the water-grain capacitors has been achieved. The conclusion by Sen (1980) and Kenyon (1984) that it is the accumulation of charge on opposite sides of platy grains that produces an increase in κ' in a fully saturated sedimentary rocks supports this type of physical model. However, we emphasize that the value of κ' for a fully saturated sandstone is essentially attained with only 2 nm of water on the pore surface; at saturations above S_w^0, there is a much more gradual and linear increase in κ' due to the addition of more bulk water in the pore space that adds relatively little to κ'.

CONCLUSIONS

The dielectric response of fully and partially saturated sandstones in the frequency range of 60 kHz to 4 MHz is determined predominantly by the presence of 2 nm of water coating the surface of the pore space. The frequency and saturation dependence of κ' suggest a conductive or Maxwell-

Wagner type of mechanism. The amount of surface water in a sandstone has been found to determine the magnitude of the frequency dependence and hence, in this frequency range, the value of κ'. The surface area-to-volume ratio of the pore space determines the amount of surface water, making this parameter (which describes the microgeometry of the pore space) the essential material property governing the dielectric response of a sandstone.

ACKNOWLEDGMENTS

We are most grateful to Mary Fitch for her assistance with data collection. We would also like to thank Les Landsberger for his part in the early stages of this project with experimental design and software development. Discussions with Ian Raistrick, Ehud Schmidt, and Dale Morgan, and the comments of Gary Olhoeft, have been very helpful and are much appreciated.

REFERENCES

Alvarez, R., 1973, Complex dielectric permittivity in rocks: a method for its measurement and analysis: Geophysics, **38**, 920–940.

Armstrong, R. D., Dickinson, T., and Whitfield, R., 1972, The impedance of the silver-solid electrolyte interface: J. Electroanal. Chem., **39**, 257–262.

Bockris, J. O'M., Gileady, E., and Muller, K., 1966, Dielectric relaxation in the electric double layer: J. Chem. Phys., **44**, 1445–1456.

Brunauer, S., Emmett, P. H., and Teller, E., 1938, Adsorption of gases in multimolecular layers: J. Am. Chem. Soc., **60**, 309–319.

Brunauer, S., Deming, L. S., Deming, W. E., and Teller, E., 1940, On a theory of the van der Waals adsorption of gases: J. Am. Chem. Soc., **62**, 1723–1732.

Cole, K. S., and Cole, R. H., 1941, Dispersion and absorption in dielectrics: J. Chem. Phys., **9**, 341–351.

Davidson, D. W., and Cole, R. H., 1951, Dielectric relaxation in glycerol, propylene glycol, and *n*-propanol: J. Chem. Phys., **29**, 1484–1490.

De Bruin, H. J., Bradwal, S. P. S., 1978, Faradaic reaction kinetics in solid electrolytes by impedance dispersion analysis: Phys. Stat. Sol. (a), **49**, K181-K184.

Debye, P., 1929, Polar molecules: Chemical Catalogue Co.

de Levie, R., 1965, The influence of surface roughness of solid electrodes on electrochemical measurements: Electrochim. Acta., **10**, 113–130.

Gast, R. G., Land, E. R., and Meyer, G. W., 1974, The interaction of water with goethite and amorphous hydrated ferric oxide surfaces: Clay and Clay Minerals, **22**, 31–39.

Grahame, D. C., 1952, Mathematical theory of the Faradaic admittance (pseudocapacity and polarization resistance): J. Electrochem. Soc., **99**, 370C-385C.

Hasted, J. B., 1961, The dielectric properties of water, *in* Birks, J. B., and Hart, J., Eds., Progress in dielectrics, **3**: John Wiley and Sons Inc., 101–149.

Hawkes, I., and Mellor, M., 1970, Uniaxial testing in rock mechanics laboratories: Eng. Geol., **4**, 177–285.

Johansen, R. T., and Dunning, H. W., 1959, Water vapour adsorption on clays: Proc., 6th National Clay Conf., 249–258.

Jonscher, A. K., 1975, The interpretation of non-ideal dielectric admittance and impedance diagrams: Phys. Stat. Solutions (a), **32**, 665–676.

——— 1979, The universal dielectric response, a review of data and their new interpretation: Chelsea Dielectrics Group, Univ. of London.

Kamiyoshi, K., and Odake, T., 1953, Dielectric properties of water adsorbed on silica gel. II dielectric dispersion of adsorbed water vapor: Science Reports of the Res. Inst. of Tohoku Univ., **A5**, 271–277.

Keller, G. V., and Licastro, P. H., 1959, Dielectric constant and electrical resistivity of natural state cores: U.S. Geol. Surv. Bull., **1052-H**, 257–285.

Kenyon, W. E., 1984, Texture effects on megahertz dielectric properties of calcite rock samples: J. Appl. Phys., **55**, 3153–3159.

Knight, R. J., 1983, The use of complex plane plots in studying the electrical response of rocks: J. Geomag. Geoelectr., **35**, 767–776.

Kurosaki, S., 1954, The dielectric behavior of water sorbed on silica gel: J. Phys. Chem., **58**, 320–324.

Lockner, D. A., and Byerlee, J. D., 1985, Complex resistivity measurements of confined rock: J. Geophys. Res., **90**, 7837–7847.

Madden, T. R., and Cantwell, T., 1967, Induced polarization, a review, *in* Musgrave, A. W., Ed., Mining geophysics, **2**, Soc. Explor. Geophys., 373–400.

Maxwell, J. C., 1891, A treatise on electricity and magnetism: Dover Publ.

McCafferty, E., and Zettlemoyer, A. C., 1971 Adsorption of water vapor on α-Fe_2O_3: Faraday Soc. Discussions, **52**, 239–254.

McIntosh, R., Rideal, E. K., Snelgrove, F.R.S., and Snelgrove, J. A., 1951, The dielectric behavior of vapours adsorbed on activated silica gel: Proc. Roy. Soc. (London), **A208**, 292–310.

Nair, N. K., and Thorp, J. M., 1965a, Dielectric behavior of water sorbed on silica gels part 1. commercial silica gels and the elimination of dieletric hysteresis: Trans., Faraday Soc., **61**, 962–974.

——— 1965b, Dielectric behavior of water adsorbed on silica gels part 2, purified silica gel and samples calcined at different temperatures: Trans., Faraday Soc., **61**, 975–989.

Olhoeft, G. R., Frisillo, A. L., and Strangway, D. W., 1974, Electrical properties of lunar soil sample 15301,38: J. Geophys. Res., **79**, 1599–1604.

Orchistron, H. D., 1955, Adsorption of water vapour: III homionic montmorillonites at 25°C: Soil Sci., **79**, 71–78.

Ormsby, W. C., and Shartsis, J. M., 1960, Surface area and exchange capacity relation in a Florida kaolinite: J. Am. Ceram. Soc., **43**, 44–47.

Pelton, W. H., Ward, S. H., Hallof, P. G., Sill, W. R., and Nelson, P. H., 1978, Mineral discrimination and removal of inductive coupling with multifrequency IP: Geophysics, **43**, 588–609.

Poley, J. Ph, Nooteboom, J. J., and de Waal, P. J., 1978, Use of v.h.f. dielectric measurements for borehole formation analysis: Log Analyst, **19**, 8–30.

Raistrick, I. D., Ho, C., and Huggins, R. A., 1976, Ionic conductivity in some lithium silicates and aluminosilicates: J. Electrochem. Soc., **123**, 1469–1476.

Raistrick, I. D., Ho, C., Hu, Y. W., and Huggins, R. A., 1977, Ionic conductivity and electrode effects on β-PbF_2: J. Electroanal. Chem., **77**, 319–337.

Saint-Amant, M., and Strangway, D. W., 1970, Dielectric properties of dry geologic materials: Geophysics, **35**, 624–645.

Sarmousakis, J. N., and Prager, M. J., 1957, Impedance at polarized platinum electrodes in various electrolytes: J. Electrochem. Soc., **104**, 454–459.

Scheider, W., 1975, Theory of the frequency dispersion of electrode polarization: topology of networks with fractional power law dependence: J. Phys. Chem., **79**, 127–136.

Scott, A. H., and Curtis, H. L., 1939, Edge correction in the determination of the dielectric constant: J. Res., National Bureau of Standards, **22**, 747–775.

Scott, J. H., Carroll, R. D., and Cunningham, D. R., 1967, Dielectric constant and electrical conductivity measurements of moist rock: a new laboratory method: J. Geophys. Res., **72**, 5105–5115.

Sen, P. N., 1980, The dielectric constant and conductivity response of sedimentary rocks: Soc. Petr. Eng., paper 9379.

Thorp, J. M., 1959, The dielectric behavior of vapours adsorbed on porous solids: Trans. Faraday Society, **55**, 442–454.

Wagner, K. W., 1914, Erklarung der dielektrischen Nachwirkungsworgange auf Grund Maxwellscher vorrstellungen: Archiv. Electrotechnik., **2**, 371.

Williams, G., and Watts, D. C., 1970, Non-symmetrical dielectric relaxation behavior arising from a simple empirical decay function: Trans., Faraday Soc., **66**, 80–85.